
Improving Importance Weighted Auto-Encoders with Annealed Importance Sampling

Xinqiang Ding*

Department of Neurobiology
The University of Chicago
Chicago, IL 60637
xqding@umich.edu

David J. Freedman

Department of Neurobiology
The University of Chicago
Chicago, IL 60637
dfreedman@uchicago.edu

Abstract

Stochastic variational inference with an amortized inference model and the reparameterization trick has become a widely-used algorithm for learning latent variable models. Increasing the flexibility of approximate posterior distributions while maintaining computational tractability is one of the core problems in stochastic variational inference. Two families of approaches proposed to address the problem are flow-based and multisample-based approaches such as importance weighted auto-encoders (IWAE). We introduce a new learning algorithm, the annealed importance weighted auto-encoder (AIWAE), for learning latent variable models. The proposed AIWAE combines multisample-based and flow-based approaches with the annealed importance sampling and its memory cost stays constant when the depth of flows increases. The flow constructed using an annealing process in AIWAE facilitates the exploration of the latent space when the posterior distribution has multiple modes. Through computational experiments, we show that, compared to models trained using the IWAE, AIWAE-trained models are better density models, have more complex posterior distributions and use more latent space representation capacity.

1 Introduction

Stochastic variational inference [1, 2, 3] is a scalable inference method for learning generative models with latent variables using stochastic optimization [4]. This method becomes especially scalable and efficient for models with continuous latent variables when it is combined with an amortized inference model and the reparameterization trick [5, 6]. The resulting method is commonly referred as the variational auto-encoder (VAE) [6]. In VAEs, a variational family of distributions parameterized by the inference model is used to approximate the posterior distribution of latent variables. VAEs learn both generative and inference models simultaneously by maximizing the evidence lower bound [5, 6]. The variational distributions used in VAEs to approximate the posterior distribution of latent variables are commonly chosen to be fully factorized, whereas the true posterior distribution is not necessarily fully factorized and might even have multiple modes. Because the optimization of generative models highly depends on the approximate posterior distribution, generative models learned using VAEs are biased toward having factorized posterior distributions and can be suboptimal.

One of the core problems in variational inference has been to increase the expressibility of approximate posterior distributions while maintaining efficient optimization [3]. Two kinds of approaches developed to address this problem are of interest for the current study: flow-based approaches [7, 8, 9] and multisample-based approaches such as the importance weighted auto-encoder (IWAE) [10].

*corresponding author

In flow-based approaches, a chain of invertible transformations, referred as a flow, is applied to samples from a simple factorized distribution such that the end samples have a more flexible distribution. Examples of flow-based approaches include normalizing flow (NF) [7], inverse autoregressive flow (IAF) [8], and the Hamiltonian variational auto-encoder (HVAE) [9] among others. Both the NF and the IAF introduce new parameters to the inference model. In contrast, the HVAE does not introduce new parameters to the inference model and the flow in HVAE is guided by the generative model. For all three flow-based approaches, calculating parameter gradients requires running the backpropagation algorithm through the flow in the reverse direction. Therefore, both computation and memory costs increase linearly with the depth of flow.

Like the HVAE, the multisample-based approach IWAE does not introduce new parameters to the inference model. The original motivation for the IWAE is to use multiple samples from an approximate posterior distribution to construct a tighter evidence lower bound and it was shown that optimizing the tighter lower bound helps learn better generative models [10]. Later, an alternative interpretation is given for the IWAE in [11, 12]. In the alternative interpretation, multiple samples from an approximate distribution are used to implicitly define a more flexible approximate posterior distribution based on importance sampling. The tighter lower bound in IWAE can be understood as a normal evidence lower bound used in VAE with the implicitly defined flexible approximate posterior distribution [11, 12].

Here we introduce the annealed importance weighted auto-encoder (AIWAE) for learning generative models with latent variables. The AIWAE combines multisample-based approaches and flow-based approaches with the annealed importance sampling and the flow used in AIWAE is constructed through an annealing process that facilitates better sampling from the posterior distribution. First, we present an alternative interpretation of how the IWAE optimizes generative model parameters: the IWAE optimizes generative model parameters by maximizing the data log-likelihood and the gradient of the data log-likelihood is estimated using importance sampling [13]. With this interpretation, we can naturally generalize the importance sampling to the annealed importance sampling (AIS) [14] to better estimate the gradient of the data log-likelihood with respect to generative model parameters. The approximate posterior distribution parameterized by the inference model and the true posterior distribution are used as the initial and the target distributions for the AIS, respectively. The inference model parameters are learned by minimizing the Kullback-Leibler (KL) divergence between the two distributions. From a flow-based point of view, samples from the initial distribution of AIS also go through a chain of transformations constructed using an annealing process. In contrast to previous flow-based approaches, the flow in AIWAE is guided by the posterior distribution and does not add new parameters to the inference model. The annealing process can facilitate the exploration of the posterior distribution when the posterior distribution has multiple modes. In addition, training models with the AIWAE does not require running the backpropagation algorithm backward through the flow and this enables the AIWAE to have a constant memory cost with the depth of the flow.

2 Background

2.1 Variational Auto-Encoder and Importance Weighted Auto-Encoder

The generative model of interest is defined by a joint distribution of both data x and continuous latent variables z : $p_\theta(x, z) = p_\theta(z)p_\theta(x|z)$, where θ represents parameters of the generative model. Learning the parameters θ by maximizing the data likelihood $p_\theta(x)$ requires calculating expectations with respect to the posterior distribution of latent variables $p_\theta(z|x)$ which is computationally expensive when analytical expressions for the expectation or $p_\theta(z|x)$ are not available. To efficiently learn the generative model, the variational auto-encoder (VAE) [5, 6] uses an approximate posterior distribution $q_\phi(z|x)$ and maximizes the evidence lower bound (ELBO) objective function $\mathcal{L}(\theta, \phi)$:

$$\mathcal{L}(\theta, \phi) = \mathbb{E}_{z \sim q_\phi(z|x)} \left[\log \frac{p_\theta(x, z)}{q_\phi(z|x)} \right] \leq \log \mathbb{E}_{z \sim q_\phi(z|x)} \left[\frac{p_\theta(x, z)}{q_\phi(z|x)} \right] = \log p_\theta(x). \quad (1)$$

The gradient of $\mathcal{L}(\theta, \phi)$ with respect to θ , $\nabla_\theta \mathcal{L}(\theta, \phi) = \mathbb{E}_{q_\phi(z|x)} [\nabla_\theta \log p_\theta(x, z)]$, is estimated by Monte Carlo sampling of z from $q_\phi(z|x)$. To efficiently estimate the gradient of $\mathcal{L}(\theta, \phi)$ with respect to ϕ , the VAE reparameterizes the approximate posterior distribution $q_\phi(z|x)$ as $z = z(\phi, x, \epsilon)$ where ϵ is a random variable from a fixed distribution and ϕ represents the parameters for the transformation. When the latent variable z is continuous, a common choice for parameterizing the approximate

posterior distribution $q_\phi(z|x)$ is $z = \mu(\phi, x) + \sigma(\phi, x) \odot \epsilon$ and $\epsilon \sim \mathcal{N}(0, \mathbf{I})$ [5, 6]. With the parameterization, the ELBO function becomes

$$\mathcal{L}(\theta, \phi) = \mathbb{E}_{\epsilon \sim \mathcal{N}(0, \mathbf{I})} \left[\log \frac{p_\theta(x, z(\phi, x, \epsilon))}{q(z(\phi, x, \epsilon)|x)} \right], \quad (2)$$

and its gradient with respect to ϕ , $\nabla_\phi \mathcal{L}(\theta, \phi)$, can be estimated by Monte Carlo sampling of ϵ from the distribution $\mathcal{N}(0, \mathbf{I})$, similarly as estimating the gradient $\nabla_\theta \mathcal{L}(\theta, \phi)$

In the importance weighted auto-encoder (IWAE) [10], the following new ELBO function based on multiple (K) samples is introduced:

$$\mathcal{L}_K(\theta, \phi) = \mathbb{E}_{z_1, \dots, z_K \sim q_\phi(z|x)} \left[\log \frac{1}{K} \sum_{k=1}^K \frac{p_\theta(x, z_k)}{q_\phi(z_k|x)} \right] \quad (3)$$

As K increases, the ELBO function $\mathcal{L}_K(\theta, \phi)$ forms a tighter lower bound of the data log-likelihood. The gradient of $\mathcal{L}_K(\theta, \phi)$ with respect to θ is

$$\nabla_\theta \mathcal{L}_K(\theta, \phi) = \mathbb{E}_{z_1, \dots, z_K \sim q_\phi(z|x)} \left[\sum_{k=1}^K \widetilde{w}_k \nabla_\theta \log w(x, z_k, \theta, \phi) \right] \quad (4)$$

$$= \mathbb{E}_{z_1, \dots, z_K \sim q_\phi(z|x)} \left[\sum_{k=1}^K \widetilde{w}_k \nabla_\theta \log p_\theta(x, z_k) \right], \quad (5)$$

where $w_k = w(x, z_k, \theta, \phi) = p_\theta(x, z_k)/q_\phi(z_k|x)$ represents the importance weight of the sample z_k and $\widetilde{w}_k = w_k / \sum_{i=1}^K w_i$ are the normalized importance weights. The gradient of $\mathcal{L}_K(\theta, \phi)$ with respect to ϕ can be calculated similarly using the reparameterization trick [10].

2.2 Importance Sampling and Annealed Importance Sampling

Importance sampling is a widely used statistical technique to compute the expectation of a function $h(z)$ with respect to a probability distribution whose density is proportional to a function $f(z)$ with an unknown normalization constant. When it is difficult to draw independent samples from the distribution $f(z)$, the importance sampling [15] uses a proposal distribution from which it is feasible to draw independent samples directly. Suppose the proposal distribution has a probability density that is proportional to $g(z)$, with the independent samples z_1, \dots, z_K drawn from the proposal distribution, the expectation $\mathbb{E}_f(h)$ can be estimated by

$$\mathbb{E}_f(h) \simeq \sum_{k=1}^K \widetilde{w}_k h(z_k) = \sum_{k=1}^K \frac{w_k}{\sum_{i=1}^K w_i} h(z_k), \quad (6)$$

where $w_k = f(z_k)/g(z_k)$ is the weight assigned for the sample z_k and $\widetilde{w}_k = w_k / \sum_{i=1}^K w_i$ is the normalized weight. The accuracy of the estimator in Eq. (6) depends on the variability of weights, $\{w_k, k = 1, \dots, K\}$, which depends on how well the proposal distribution defined by $g(z)$ can approximate the target distribution defined by $f(z)$. When z is high dimensional and $f(z)$ is complex and has multiple modes, it is difficult to identify the proposal distribution which is not only a good approximation of the target distribution, but also easy to draw independent samples from.

An alternative approach is to use Markov chain Monte Carlo (MCMC) approaches [15] to draw dependent samples from the target distribution defined by $f(z)$. This works by making random perturbations to samples and accepting or rejecting the perturbed samples based on the Metropolis-Hastings criterion [16, 17]. Although theoretical results show that, under relatively weak conditions, the samples will eventually converge to the target distribution [15], this might necessitate running the Markov chain for too long to be practical, especially when the target distribution has multiple modes that are connected only through low density regions.

The annealed importance sampling (AIS) [14] was introduced to alleviate challenges evident in both importance sampling and MCMC. In AIS, a sequence of distributions with probability densities proportional to $f_1(z), \dots, f_{n-1}(z)$ are constructed to connect the initial distribution defined

by $f_0(z) = g(z)$ and the target distribution defined by $f_n(z) = f(z)$. A generally useful way to construct these intermediate distributions is to let

$$f_t(z) = f_0(z)^{1-\beta_t} f_n(z)^{\beta_t}, \quad (7)$$

where $0 = \beta_0 < \beta_1 < \dots < \beta_{n-1} < \beta_n = 1$. To generate a sample z_k and calculate its weight w_k , a sequence of samples $\{z^0, \dots, z^n\}$ is generated as follows. Initially, z^0 is generated by sampling from the distribution $f_0(z)$, which is chosen to be a distribution from which independent samples can be easily drawn. For $1 \leq t \leq n$, z^t is generated using a reversible transition kernel $T_t(z|z^{t-1})$ that keeps f_t invariant. Then the sample z_k is set to $z_k = z^n$ and the weight w_k is calculated as:

$$w_k = \frac{f_1(z^0) f_2(z^1) \dots f_{n-1}(z^{n-2}) f_n(z^{n-1})}{f_0(z^0) f_1(z^1) \dots f_{n-2}(z^{n-2}) f_{n-1}(z^{n-1})}. \quad (8)$$

After generating samples z_1, \dots, z_K and their weights w_1, \dots, w_K , the expectation $\mathbb{E}_f(h)$ can be similarly estimated using Eq. (6).

3 Annealed Importance Weighted Autoencoders

In this section, we introduce the annealed importance weighted auto-encoder (AIWAE) for learning the generative model $p_\theta(x, z)$ by maximizing the data log-likelihood $\log p_\theta(x)$. The AIWAE originates from the importance sampling interpretation of the gradient $\nabla_\theta \mathcal{L}_k(\theta, \phi)$ in Eq. (5). With this interpretation, Eq. (5) can be naturally generalized to utilize the AIS [14].

Let us consider learning parameters θ for the generative model $p_\theta(x, z)$ by maximizing the data log-likelihood with stochastic gradient ascent. In order to do that, we need to estimate the gradient of the data log-likelihood $\log p_\theta(x)$ with respect to θ :

$$\nabla_\theta \log p_\theta(x) = \mathbb{E}_{z \sim p_\theta(z|x)} [\nabla_\theta \log p_\theta(x, z)]. \quad (9)$$

Because directly drawing independent samples from the posterior distribution $p_\theta(z|x)$ is usually not feasible, we can use the importance sampling approach to estimate the above expectation. If we choose the proposal distribution is to be $q_\phi(z|x)$, then setting $f(z) = p_\theta(z|x)$ and $g(z) = q_\phi(z|x)$ in Eq. (6) yields the following estimator:

$$\nabla_\theta \log p_\theta(x) \simeq \sum_{k=1}^K \widetilde{w}_k \nabla_\theta \log p_\theta(x, z_k), \quad (10)$$

where $\widetilde{w}_k = w_k / \sum_{i=1}^K w_i$ and $w_k = w(x, z_k, \theta, \phi) = p_\theta(x, z_k) / q_\phi(z_k|x)$. This estimator (Eq. 10) is the same as the estimator in Eq. (5) that is used to estimate the gradient of the ELBO function $\nabla_\theta \mathcal{L}_k(\theta, \phi)$. Therefore, in terms of learning the parameter θ , an alternative interpretation of the IWAE is that it learns the parameter θ by maximizing the data log-likelihood $\log p_\theta(x)$ and the gradient $\nabla_\theta \log p_\theta(x)$ is estimated using importance sampling with the approximate posterior distribution as the proposal distribution.

With the importance sampling view, the estimator in Eq. (10) can be improved using the AIS [14] as follows. The unnormalized density $f_n(z)$ for the target distribution is set to $f_n(z) = p_\theta(x, z)$ and the initial distribution density $f_0(z)$ is set to $f_0(z) = q_\phi(z|x)$. A sequence of intermediate distributions is constructed using Eq. (7), i.e., $f_t(z) = q_\phi(z|x)^{1-\beta_t} p_\theta(x, z)^{\beta_t}$. The reversible transition kernel $T_t(z|z^{t-1})$ that leaves $f_t(z)$ invariant is constructed using the Hamiltonian Monte Carlo (HMC) method [18] in which the potential energy function $U_t(z)$ is set to $U_t(z) = -\log f_t(z)$. With the estimation of the gradient $\nabla_\theta \log p_\theta(x)$ (Eq. 10) using AIS, we can optimize the parameter θ by maximizing the data log-likelihood $\log p_\theta(x)$ with stochastic gradient ascent.

The importance sampling interpretation of Eq. (5) and the optimization procedure using AIS to estimate gradients of data log-likelihood only apply to the parameter θ of the generative model $p_\theta(x, z)$. How should we optimize the parameter ϕ in the approximate inference model $q_\phi(z|x)$? In the AIWAE, we take the following general strategy. The main objective of AIWAE is to learn the generative model $p_\theta(x, z)$ by maximizing the data log-likelihood. It requires calculating the expectation with respect to the posterior distribution $p_\theta(z|x)$, i.e., $\mathbb{E}_{z \sim p_\theta(z|x)} [\nabla_\theta \log p_\theta(x, z)]$. The amortized approximate inference model $q_\phi(z|x)$ is introduced to help efficiently estimate the expectation. Because the performance of AIS estimation depends on the similarity between its initial

and target distributions, the objective in optimizing the parameters ϕ is to make $q_\phi(z|x)$ become close to the posterior distribution $p_\theta(z|x)$. In AIWAE, we choose to minimize the Kullback-Leibler divergence between $q_\phi(z|x)$ and $p_\theta(z|x)$, i.e., maximize the ELBO function $\mathcal{L}(\theta, \phi)$ (Eq. (2)) with the reparameterization trick as in VAE [6]. Overall, the detailed procedures of the AIWAE are described in Algorithm (1).

Algorithm 1: Annealed Importance Weighted Auto-Encoder

Require:

x : a data point

K : the number of annealed importance weighted samples

Generative and Inference Models

$p_\theta(x, z)$: the joint distribution density of the generative model

$q_\phi(z|x)$: the approximate posterior distribution density

Parameters for Hamiltonian Monte Carlo (HMC)

T : the number of inverse temperatures

$\{\beta_t : t = 0, \dots, T-1, 0 = \beta_0 < \dots < \beta_{T-1} = 1\}$: inverse temperatures

$\{\epsilon_t : t = 1, \dots, T-1\}$: the step size used in leapfrog integration at each inverse temperature

L : the number of integration steps

Calculate Gradients and Optimize Parameters:

while θ, ϕ not converged **do**

sample example(s) x from the training data;

update the generative model parameter θ

set $\log w_k = 0$ for $k = 1, \dots, K$;

sample $z^0 = [z_1^0, z_2^0, \dots, z_K^0]$, where z_k^0 are i.i.d. samples from $q_\phi(z|x)$;

for $t \leftarrow 1$ **to** $T-1$ **do**

$\log w_k \leftarrow \log w_k + (\beta_t - \beta_{t-1})[\log p_\theta(x, z_k^{t-1}) - \log q_\phi(z_k^{t-1}|x)]$ for $k = 1, \dots, K$;

$z^t = \text{HMC}(z^{t-1}, \beta_t, \epsilon_t, L)$, where the potential energy function is:

$$U_t(z) = -\log f_t(z) \text{ and } f_t(z) = q_\phi(z|x)^{1-\beta_t} p_\theta(x, z)^{\beta_t};$$

set $z = [z_1, \dots, z_K] = [z_1^{T-1}, \dots, z_K^{T-1}]$ and $\tilde{w}_k = w_k / \sum_{i=1}^K w_i$;

estimate the gradient $\nabla_\theta \log p_\theta(x)$ with $\delta_\theta = \sum_{k=1}^K \tilde{w}_k \nabla_\theta \log p_\theta(x, z_k)$;

apply gradient update to θ using δ_θ ;

update the inference model parameter ϕ

sample $\epsilon \sim \mathcal{N}(0, \mathbf{I})$;

set $z = \mu(\phi, x) + \sigma(\phi, x) \odot \epsilon$ and calculate $\mathcal{L}(\theta, \phi)$;

estimate the gradient $\delta_\phi = \nabla_\phi \mathcal{L}(\theta, \phi)$ with the reparameterization trick;

apply gradient update to ϕ using δ_ϕ ;

In summary, the parameters θ and ϕ are optimized using different objective functions in AIWAE. The generative model parameters θ are optimized to maximize the data log-likelihood and the inference model parameters ϕ are optimized to maximize the ELBO (Eq. 2) function with the reparameterization trick. The purpose of the inference model is to help efficiently calculate the gradient of the data log-likelihood with respect to θ (Eq. (9)). When the posterior distribution $p_\theta(z|x)$ is not factorized and has multiple modes, the fully factorized approximate posterior distribution $q_\phi(z|x)$ will not be a good approximation and the estimator based on importance sampling with $q_\phi(z|x)$ (Eq. (10)) will have a large variance. AIS is used to alleviate this problem. With AIS, samples from the approximate distribution $q_\phi(z|x)$ are transformed via an annealing process guided by the posterior distribution $p_\theta(z|x)$ such that the distribution of these samples moves towards $p_\theta(z|x)$. The annealing procedure in AIS can also help samples explore when $p_\theta(z|x)$ has multiple modes. In contrasted to other flow-based approaches, the AIWAE's memory cost does not increase with the depth of flow. The computational cost of AIWAE is proportional to both the number of weighted samples K and the number of steps $T \times L$ in the flow, whereas the computational cost of IWAE is only proportional to K . Therefore, AIWAE is approximately $T \times L$ times more expensive than IWAE in computation when the same K is used.

4 Related Work

In addition to the IWAE and AIWAE, several approaches have been proposed to utilize multiple samples with importance sampling to either obtain a better objective function or to better estimate gradients of objective functions. For learning feedforward neural networks with stochastic binary hidden units, an importance sampling based estimator using multiple samples was proposed in [19] to estimate the expectation used in the generalized Expectation-Maximization algorithm [20]. A similar estimator was derived in [21] by constructing a variational distribution of hidden variables used in ELBO using multiple samples and importance sampling. Another approach [22] extended the multisample approach in IWAE to discrete latent variables and developed an unbiased gradient estimator for importance-sampled objectives. Methods in [19, 21, 22] apply for models with discrete latent variables, whereas the IWAE only applies for models with continuous latent variables. Although our current extension of IWAE to AIWAE using AIS also only applies for continuous latent variables, the idea of replacing importance sampling with AIS could also be useful for improving methods in [19, 21, 22] that work for discrete latent variables.

The reweighted wake-sleep (RWS) algorithm [13] is another multisample approach for learning generative models with latent variables. Different from the IWAE, the RWS algorithm uses different objective functions for optimizing the generative and the inference models. The generative model is optimized by maximizing the data log-likelihood with its gradient estimated using importance sampling. This gradient estimator is equivalent to the gradient estimator of $\nabla_{\theta} \mathcal{L}_K(\theta, \phi)$ (Eq. (5)) in IWAE. To optimize the inference model, two different update rules were proposed in RWS: (1) (wake phase update) minimizing the Kullback-Leibler divergence between $p_{\theta}(z|x)$ and $q_{\phi}(z|x)$ $D_{\text{KL}}(p_{\theta}(z|x)||q_{\phi}(z|x))$ with the gradient estimated using importance sampling; (2) (sleep phase update) maximizing the log-likelihood $q_{\phi}(z|x)$ for samples (x, z) from $p_{\theta}(x, z)$. Compared with the RWS, the AIWAE is different in two aspects: (1) instead of importance sampling, the AIS is used to estimate $\nabla_{\theta} \log p_{\theta}(x)$ when optimizing the generative model; (2) the inference model is optimized by minimizing $D_{\text{KL}}(q_{\phi}(z|x)||p_{\theta}(z|x))$ using the reparameterization trick. It will be interesting to investigate if replacing importance sampling with AIS can also help RWS learn better generative models.

The AIWAE utilizes both MCMC and variational inference. In this respect, one closely related approach is that proposed in [23], which uses the same objective functions as AIWAE for both generative and inference models. The difference between AIWAE and [23] is in the method for approximating the gradient $\nabla_{\theta} \log p_{\theta}(x) = \mathbb{E}_{z \sim p_{\theta}(z|x)}[\nabla_{\theta} \log p_{\theta}(x, z)]$ (Eq. (9)). In [23], only one approximate sample from $p_{\theta}(z|x)$ is used to approximate the expectation $\mathbb{E}_{z \sim p_{\theta}(z|x)}[\nabla_{\theta} \log p_{\theta}(x, z)]$ for each data point x . The approximate sample is generated by first sampling from the approximate distribution $q_{\phi}(z|x)$ and then applying multiple Hamiltonian Monte Carlo (HMC) steps to the sample. In the HMC steps, the energy function is set to be $U(z) = -\log p_{\theta}(x, z)$. When the distribution $p_{\theta}(z|x)$ has multiple modes, running HMC for a limited number of steps with $U(z) = -\log p_{\theta}(x, z)$ can be difficult for exploring multiple modes. Multimodal distribution is less of a problem for AIWAE because the annealing process in AIS starts with the smooth energy function $U(z) = -\log q_{\phi}(z|x)$ and slowly switches into the rugged energy function $U(z) = \log p_{\theta}(x, z)$.

The Hamiltonian variational inference (HVI) [24] is another related approach combining MCMC and variational inference. Different from both AIWAE and [23], HVI considers samples from HMC steps as auxiliary variables and optimizes a single objective function called the auxiliary variational lower bound. A disadvantage of HVI is that it is required to learn an extra inference network for auxiliary variables to reverse the transformations in HMC steps, which introduces new parameters. In addition, learning the auxiliary variables also requires running the backpropagation algorithm backward through the HMC transformations, which increases the memory cost linearly with the number of HMC steps.

5 Experiments

5.1 Dataset and Model Setup

We conducted a series of experiments to evaluate the performance of AIWAE on learning generative models using both the MNIST [25] dataset and the Omniglot dataset [26]. The same generative models are also learned using IWAE and the performance of IWAE is compared to that of AIWAE.

We used the same generative model and the same inference model as that used in the IWAE study [10]. The dimension of the latent variable z is 50. For the generative model $p_\theta(x, z) = p(z)p_\theta(x|z)$, the prior distribution $p(z)$ is a 50 dimensional standard Gaussian distribution. The conditional distribution $p_\theta(x|z)$ is a Bernoulli distribution and is parameterized by a neural network with two hidden layers, each of which has 200 units. The approximate posterior distribution $q_\phi(z|x)$ is a 50 dimensional Gaussian distribution with a diagonal covariance matrix. Its mean $\mu(x)$ and variance $\sigma(x)$ are similarly parameterized by a neural network with two hidden layers. We used the same optimization procedure [27] as that used in the IWAE study. The detailed information about the datasets, model setup and optimization is included in the supplementary material.

Models were trained using both IWAE and AIWAE with different hyperparameters. For both IWAE and AIWAE, the number of importance weighted samples K is set to 1, 5 or 50. As shown in Algorithm (1), extra hyperparameters are required for the AIWAE. For each $K \in \{1, 5, 50\}$, the number of inverse temperatures T is set to 5, 8, or 11. Given a $T \in \{5, 8, 11\}$, the inverse temperatures β_t are evenly distributed between 0 and 1, i.e., $\beta_t = t/(T - 1)$ for $i = 0, \dots, T - 1$. In HMC, the number of integration steps L is set to 5 and the step sizes ϵ_t are dynamically adapted such that the acceptance ratio is close to 0.6.

5.2 Results

Table 1: Results of both AIWAE and IWAE on the MNIST dataset

K	1				5				50			
	IWAE	AIWAE			IWAE	AIWAE			IWAE	AIWAE		
		T = 5	T = 8	T = 11		T = 5	T = 8	T = 11		T = 5	T = 8	T = 11
NLL(test)	86.07	84.55	84.31	84.19	85.17	84.23	84.06	83.90	84.13	83.92	83.79	83.68
NLL(train)	85.89	84.59	84.35	84.15	84.93	84.26	84.12	83.96	83.95	83.96	83.84	83.81
NVLB(test)	86.60	87.30	87.79	88.02	85.64	88.11	88.95	89.59	84.77	89.24	90.44	91.55
NVLB(train)	86.26	87.22	87.72	87.94	85.31	88.02	88.88	89.45	84.42	89.17	90.28	91.41
var gap	0.53	2.75	3.48	3.83	0.47	3.89	4.89	5.68	0.63	5.32	6.65	7.87
gen gap	0.18	-0.04	-0.04	0.05	0.24	-0.04	-0.06	-0.05	0.18	-0.04	-0.05	-0.13
active units	18	28	31	32	20	32	34	35	23	35	38	40

Table 2: Results of both AIWAE and IWAE on the Omniglot dataset

K	1				5				50			
	IWAE	AIWAE			IWAE	AIWAE			IWAE	AIWAE		
		T = 5	T = 8	T = 11		T = 5	T = 8	T = 11		T = 5	T = 8	T = 11
NLL(test)	107.39	103.23	102.63	102.43	105.30	102.54	102.10	102.05	103.31	102.07	101.83	101.68
NLL(train)	105.75	101.47	100.85	100.60	103.45	100.71	100.33	100.14	101.29	100.18	99.89	99.71
NVLB(test)	108.19	107.51	108.47	109.17	106.30	108.60	109.81	110.46	104.67	109.89	110.96	111.88
NVLB(train)	106.32	105.37	106.20	106.78	104.14	106.38	107.43	108.02	102.36	107.46	108.33	109.20
var gap	0.79	4.28	5.84	6.74	1.00	6.06	7.72	8.42	1.36	7.82	9.13	10.20
gen gap	1.65	1.76	1.78	1.83	1.85	1.83	1.77	1.90	2.02	1.90	1.94	1.97
active units	27	47	50	50	32	50	50	50	39	50	50	50

Models trained with both IWAE and AIWAE with different hyperparameters are first evaluated using negative data log-likelihoods (NLLs) and negative variational lower bounds (NVLBs). Following [28], NLLs are calculated using 16 independent AIS chains with 10,000 inverse temperatures evenly spaced between 0 and 1. HMC with 10 leapfrog steps is used as the transition kernel and the leapfrog step size is tuned to achieve an acceptance ratio of 0.6. Following the IWAE study, NVLBs are calculated as $-\mathcal{L}_{5000}$ (Eq. 3).

Results on the MNIST dataset and the Omniglot dataset are presented in Table (3) and Table (4), respectively. Each experiment was repeated for 5 times and results shown in Table (3 and 4) are mean values (standard derivations are included in the tables in supplementary material). For IWAE with $K \in \{1, 5, 50\}$, the values of NVLB agree with that in the IWAE study. As the number of importance weighted samples K increases from 1 to 50, the generative model trained with IWAE improves because the values of NLLs decrease. For a fixed $K \in \{1, 5, 50\}$, models trained with AIWAE have lower values of NLLs than models trained with IWAE for all choices of $T \in \{5, 8, 11\}$. Therefore,

AIWAE produces better density models than IWAE. In addition, as the number of inverse temperature T increases from 5 to 11 in AIWAE, the resulting density models improve further. Similar to IWAE, models trained with AIWAE with a fixed T also improve when the number of annealed weighted samples K increases.

When $K = 50$ and $T = 11$, the model trained with AIWAE achieves a log-likelihood of -83.68 and -101.68 on the MNIST dataset and the Omniglot dataset, respectively. We note that these results are for permutation-invariant models with only one stochastic layer. For the Omniglot dataset, our best result with a log-likelihood of -101.68 is better than the best result in the IWAE study which has an approximate log-likelihood of -103.38 and is obtained with two stochastic layers [10]. The generalization ability of the models is quantified by the generalization gap (gen gap in Table (3 and 4)) which is defined as the difference between the log-likelihood values on test and training data. For the MNIST dataset, models trained with both IWAE and AIWAE have quite small generalization gaps (smaller than 0.25 nats). Most of the models trained with AIWAE have generalization gaps that are not significantly different from 0 nats.

In both VAE and IWAE, a factorized approximate posterior distribution is used to approximate the posterior distribution $p_\theta(z|x)$ and the generative model $p_\theta(x, z)$ is trained by optimizing the ELBO objective function. In this kind of optimization, the generative model $p_\theta(x, z)$ is biased such that the posterior distribution $p_\theta(z|x)$ is approximately factorized. Alleviating the bias is the main motivation for replacing importance sampling used in IWAE with AIS in AIWAE. Here we use the variational gap (var gap in Table (3 and 4)), defined as $\log p_\theta(x) - \mathcal{L}_{5000}(\theta, \phi)$, to quantify the bias. Results show that models trained with AIWAE have greater variational gaps than those trained with IWAE. This means that posterior distributions $p_\theta(z|x)$ of models trained with AIWAE are more different from factorized distributions than are posterior distributions of models trained with IWAE. Therefore, the generative models trained with AIWAE are less biased towards having factorized posterior distribution and have more complex structures in the posterior distribution. For models trained with AIWAE, as the number of annealed importance weighted samples K or the number of inverse temperatures T increases, the NLLs decrease whereas the NVLBs increase. This makes the variational gaps increases as either K or T increases. This implies that, as K and T increase, models learned with AIWAE not only become better on density estimation but also have more complex posterior distributions. (A visualization of posterior distributions for models learned with both IWAE and AIWAE is included in supplementary material when the dimension of z is set to 2.)

Following the IWAE study[10], we also calculated the number of active latent units and used it to represent how much the latent space’s representation capacity was utilized in learned models. The intuition is that if a latent unit is active for encoding information in the observation, it is expected that its distribution would change with observations. Therefore, we used the following variance statistics to quantify the activity of the a latent unit h : $A_h = \text{Cov}_{x \in \text{test set}}(\mathbb{E}_{h \sim q(h|x)}[h])$, which measures how much the value of a latent unit changes when the observation in test set changes. A latent unit h is defined to be active if $A_h > 10^{-2}$. Both the statistics A_h and the cutoff value are adopted from the IWAE study [10]. As shown in both Table (3 and 4), the number of active units in models trained with AIWAE is much larger than that in models trained with IWAE. In addition, the number of active units in models trained with AIWAE increases monotonically not only with the number of samples but also with the number of inverse temperatures. Intuitively, when the number of inverse temperature increases, the annealing process in AIWAE becomes longer and smoother, making it easier for samples to explore more latent space. On the Omniglot dataset, all the latent units are active for most of the models trained with AIWAE.

6 Conclusion

We present the annealed importance weighted auto-encoder (AIWAE), a learning algorithm for training probabilistic generative models with latent variables. AIWAE combines multisample-based and flow-based approaches with the annealed importance sampling to better approximate the posterior distribution. In contrast with previous flow-based approaches, AIWAE does not require running backpropagation backwards through flows and has constant memory cost with the depth of flows. AIWAE can also be viewed as a way of combining MCMC with variational inference or trading learning speed for model accuracy. The annealed sampling process used in AIWAE facilitates sampling from complex posterior distributions. In experiments, we demonstrate that, compared with

models learned with IWAE, models learned with AIWAE have higher likelihood on data, have more complex posterior distribution and utilize more of their latent space representational capacity.

References

- [1] Martin J Wainwright, Michael I Jordan, et al. Graphical models, exponential families, and variational inference. *Foundations and Trends® in Machine Learning*, 1(1–2):1–305, 2008.
- [2] Matthew D Hoffman, David M Blei, Chong Wang, and John Paisley. Stochastic variational inference. *The Journal of Machine Learning Research*, 14(1):1303–1347, 2013.
- [3] David M Blei, Alp Kucukelbir, and Jon D McAuliffe. Variational inference: A review for statisticians. *Journal of the American Statistical Association*, 112(518):859–877, 2017.
- [4] Herbert Robbins and Sutton Monro. A stochastic approximation method. *The annals of mathematical statistics*, pages 400–407, 1951.
- [5] Danilo Jimenez Rezende, Shakir Mohamed, and Daan Wierstra. Stochastic backpropagation and approximate inference in deep generative models. *arXiv preprint arXiv:1401.4082*, 2014.
- [6] Diederik P Kingma and Max Welling. Auto-encoding variational bayes. *arXiv preprint arXiv:1312.6114*, 2013.
- [7] Danilo Jimenez Rezende and Shakir Mohamed. Variational inference with normalizing flows. *arXiv preprint arXiv:1505.05770*, 2015.
- [8] Durk P Kingma, Tim Salimans, Rafal Jozefowicz, Xi Chen, Ilya Sutskever, and Max Welling. Improved variational inference with inverse autoregressive flow. In *Advances in neural information processing systems*, pages 4743–4751, 2016.
- [9] Anthony L Caterini, Arnaud Doucet, and Dino Sejdinovic. Hamiltonian variational auto-encoder. In *Advances in Neural Information Processing Systems*, pages 8167–8177, 2018.
- [10] Yuri Burda, Roger Grosse, and Ruslan Salakhutdinov. Importance weighted autoencoders. *arXiv preprint arXiv:1509.00519*, 2015.
- [11] Chris Cremer, Quaid Morris, and David Duvenaud. Reinterpreting importance-weighted autoencoders. *arXiv preprint arXiv:1704.02916*, 2017.
- [12] Philip Bachman and Doina Precup. Training deep generative models: Variations on a theme. In *NIPS Approximate Inference Workshop*, 2015.
- [13] Jörg Bornschein and Yoshua Bengio. Reweighted wake-sleep. *arXiv preprint arXiv:1406.2751*, 2014.
- [14] Radford M Neal. Annealed importance sampling. *Statistics and computing*, 11(2):125–139, 2001.
- [15] Christian Robert and George Casella. *Monte Carlo statistical methods*. Springer Science & Business Media, 2013.
- [16] Nicholas Metropolis, Arianna W Rosenbluth, Marshall N Rosenbluth, Augusta H Teller, and Edward Teller. Equation of state calculations by fast computing machines. *The journal of chemical physics*, 21(6):1087–1092, 1953.
- [17] W. K. Hastings. Monte Carlo sampling methods using Markov chains and their applications. *Biometrika*, 57(1):97–109, 04 1970.
- [18] Radford M Neal et al. Mcmc using hamiltonian dynamics. *Handbook of markov chain monte carlo*, 2(11):2, 2011.
- [19] Yichuan Tang and Ruslan R Salakhutdinov. Learning stochastic feedforward neural networks. In *Advances in Neural Information Processing Systems*, pages 530–538, 2013.
- [20] Radford M Neal and Geoffrey E Hinton. A view of the em algorithm that justifies incremental, sparse, and other variants. In *Learning in graphical models*, pages 355–368. Springer, 1998.
- [21] Tapani Raiko, Mathias Berglund, Guillaume Alain, and Laurent Dinh. Techniques for learning binary stochastic feedforward neural networks. *arXiv preprint arXiv:1406.2989*, 2014.
- [22] Andriy Mnih and Danilo J Rezende. Variational inference for monte carlo objectives. *arXiv preprint arXiv:1602.06725*, 2016.

- [23] Matthew D Hoffman. Learning deep latent gaussian models with markov chain monte carlo. In *Proceedings of the 34th International Conference on Machine Learning-Volume 70*, pages 1510–1519. JMLR. org, 2017.
- [24] Tim Salimans, Diederik Kingma, and Max Welling. Markov chain monte carlo and variational inference: Bridging the gap. In *International Conference on Machine Learning*, pages 1218–1226, 2015.
- [25] Yann LeCun, Léon Bottou, Yoshua Bengio, Patrick Haffner, et al. Gradient-based learning applied to document recognition. *Proceedings of the IEEE*, 86(11):2278–2324, 1998.
- [26] Brenden M Lake, Ruslan Salakhutdinov, and Joshua B Tenenbaum. Human-level concept learning through probabilistic program induction. *Science*, 350(6266):1332–1338, 2015.
- [27] Diederik P Kingma and Jimmy Ba. Adam: A method for stochastic optimization. *arXiv preprint arXiv:1412.6980*, 2014.
- [28] Yuhuai Wu, Yuri Burda, Ruslan Salakhutdinov, and Roger Grosse. On the quantitative analysis of decoder-based generative models. *arXiv preprint arXiv:1611.04273*, 2016.

Supplementary Material

A Details about datasets, model setup and optimization

In the MNIST dataset, there are 60,000 training examples and 10,000 test examples. In the Omniglot dataset, there are 24,345 training examples and 8,070 test examples². Images from both datasets have a dimension of 28×28 . For both training and testing, images are dynamically binarized into vectors of 0 and 1 with the probability of being 1 equal to normalized pixel values between 0 and 1.

We used the same generative model and the same inference model as that used in the IWAE study. The dimension of the latent variable z is 50. For the generative model $p_\theta(x, z) = p(z)p_\theta(x|z)$, the prior distribution $p(z)$ is a 50 dimensional standard Gaussian distribution. The generative conditional distribution $p_\theta(x|z)$ is a Bernoulli distribution. The probability p of the Bernoulli distribution is parameterized by the following neural network with two hidden layers: $h_1 = \tanh(W_1 z + b_1)$, $h_2 = \tanh(W_2 h_1 + b_2)$, $p = \text{sigmoid}(W_3 h_2 + b_3)$, where both h_1 and h_2 have 200 units and p has 784 units. The approximate posterior distribution $q_\phi(z|x)$ is a 50 dimensional Gaussian distribution with a diagonal covariance matrix. Its mean $\mu(x)$ and variance $\sigma(x)$ are similarly parameterized by the following neural network with two hidden layers: $h_1 = \tanh(W_1 x + b_1)$, $h_2 = \tanh(W_2 h_1 + b_2)$, $\mu(x) = W_3 h_2 + b_3$, $\sigma(x) = \exp(W_4 h_2 + b_4)$, where both h_1 and h_2 have 200 units.

We used the same optimization setup as that used in the IWAE study. The Adam optimizer is used with parameters $\beta_1 = 0.9$, $\beta_2 = 0.999$, and $\epsilon = 10^{-4}$. The optimization was preceeded for 3^i passes over the data with a learning rate of $0.001 \cdot 10^{-i/7}$ for $i = 0, \dots, 7$. Overall, the optimization was run for 3,280 epochs. For IWAE, the size of a minibatch is 20 which is the same as that in the IWAE study. For AIWAE, the minibatch size is set to 128 to accelerate training.

B Performance of models trained with both AIWAE and IWAE on both the MNIST and the Omniglot dataset when the dimension of latent variable z is equal to 50

Each experiment was repeated for 5 times. The results shown in Table (3 and 4) are mean values from the 5 repeats. Values in parentheses are standard deviations.

²The Omniglot data was downloaded from <https://github.com/yburda/iwae.git>

Table 3: Results of both AIWAE and IWAE on the MNIST dataset

K	5						50					
	1			5			1			5		
	IWAE		AIWAE	IWAE		AIWAE	IWAE		AIWAE	IWAE		AIWAE
	T=5	T=8	T=11	T=5	T=8	T=11	T=5	T=8	T=11	T=5	T=8	T=11
NLL(test)	86.07 (0.07)	84.55 (0.07)	84.31 (0.08)	84.19 (0.06)	85.17 (0.10)	84.23 (0.10)	84.06 (0.05)	83.90 (0.03)	84.13 (0.06)	83.92 (0.07)	83.79 (0.06)	83.68 (0.10)
NLL(train)	85.89 (0.07)	84.59 (0.09)	84.35 (0.06)	84.15 (0.07)	84.93 (0.06)	84.26 (0.08)	84.12 (0.05)	83.96 (0.04)	83.95 (0.06)	83.96 (0.05)	83.84 (0.09)	83.81 (0.09)
NVLB(test)	86.60 (0.07)	87.30 (0.08)	87.79 (0.17)	88.02 (0.17)	85.64 (0.09)	88.11 (0.15)	88.95 (0.18)	89.59 (0.27)	84.77 (0.05)	89.24 (0.21)	90.44 (0.50)	91.55 (1.15)
NVLB(train)	86.26 (0.05)	87.22 (0.08)	87.72 (0.12)	87.94 (0.15)	85.31 (0.06)	88.02 (0.13)	88.88 (0.15)	89.45 (0.26)	84.42 (0.03)	89.17 (0.21)	90.28 (0.47)	91.41 (1.16)
var gap	0.53 (0.06)	2.75 (0.08)	3.48 (0.11)	3.83 (0.21)	0.47 (0.10)	3.89 (0.17)	4.89 (0.20)	5.68 (0.26)	0.63 (0.09)	5.32 (0.23)	6.65 (0.45)	7.87 (1.06)
gen gap	0.18 (0.08)	-0.04 (0.04)	-0.04 (0.07)	0.05 (0.03)	0.24 (0.10)	-0.04 (0.06)	-0.06 (0.06)	-0.05 (0.03)	0.18 (0.01)	-0.04 (0.04)	-0.05 (0.05)	-0.13 (0.02)
active units	18	28	31	32	20	32	34	35	23	35	38	40

Table 4: Results of both AIWAE and IWAE on the Omniglot dataset

K	50											
	1					5						
	IWAE		AIWAE		IWAE	AIWAE		IWAE	AIWAE		IWAE	
	T=5	T=8	T=11	T=5		T=8	T=11		T=5	T=8		T=11
NLL(test)	107.39 (0.16)	103.23 (0.07)	102.63 (0.09)	102.43 (0.11)	105.30 (0.07)	102.54 (0.08)	102.10 (0.07)	102.05 (0.06)	103.31 (0.09)	102.07 (0.08)	101.83 (0.07)	101.68 (0.09)
NLL(train)	105.75 (0.11)	101.47 (0.06)	100.85 (0.10)	100.60 (0.10)	103.45 (0.06)	100.71 (0.05)	100.33 (0.04)	100.14 (0.08)	101.29 (0.06)	100.18 (0.06)	99.89 (0.08)	99.71 (0.06)
NVLB(test)	108.19 (0.16)	107.51 (0.07)	108.47 (0.08)	109.17 (0.10)	106.30 (0.04)	108.60 (0.14)	109.81 (0.10)	110.46 (0.14)	104.67 (0.12)	109.89 (0.15)	110.96 (0.12)	111.88 (0.14)
NVLB(train)	106.32 (0.13)	105.37 (0.06)	106.20 (0.08)	106.78 (0.15)	104.14 (0.04)	106.38 (0.11)	107.43 (0.07)	108.02 (0.12)	102.36 (0.04)	107.46 (0.10)	108.33 (0.11)	109.20 (0.13)
var gap	0.79 (0.03)	4.28 (0.08)	5.84 (0.10)	6.74 (0.08)	1.00 (0.06)	6.06 (0.10)	7.72 (0.12)	8.42 (0.14)	1.36 (0.06)	7.82 (0.08)	9.13 (0.14)	10.20 (0.06)
gen gap	1.65 (0.10)	1.76 (0.03)	1.78 (0.07)	1.83 (0.05)	1.85 (0.05)	1.83 (0.04)	1.77 (0.06)	1.90 (0.04)	2.02 (0.05)	1.90 (0.04)	1.94 (0.09)	1.97 (0.03)
active units	27	47	50	50	32	50	50	50	39	50	50	50

C Posterior distributions $p_\theta(z|x)$ of models trained with both AIWAE and IWAE on the MNIST dataset when the dimension of z is equal to 2

In order to visualize the posterior distribution $p_\theta(z|x)$, we also trained models with the dimension of z being 2 using both AIWAE and IWAE on the MNIST dataset. Other model setup and the optimization procedure are the same as those used for models with the dimension of z being 50.

Figures S0-S9 show posterior distributions $p_\theta(z|x)$ of models trained with both IWAE and AIWAE for examples of digits 0-9. The first row represents models learned with IWAE and the second to the last row represents models learned with AIWAE using different numbers of temperature. The left, middle, and right columns represents models learned with 1, 5, and 50 samples, respectively. The digits used for calculating the posterior distributions shown in Figures S0-S9 are shown in Figure S10.

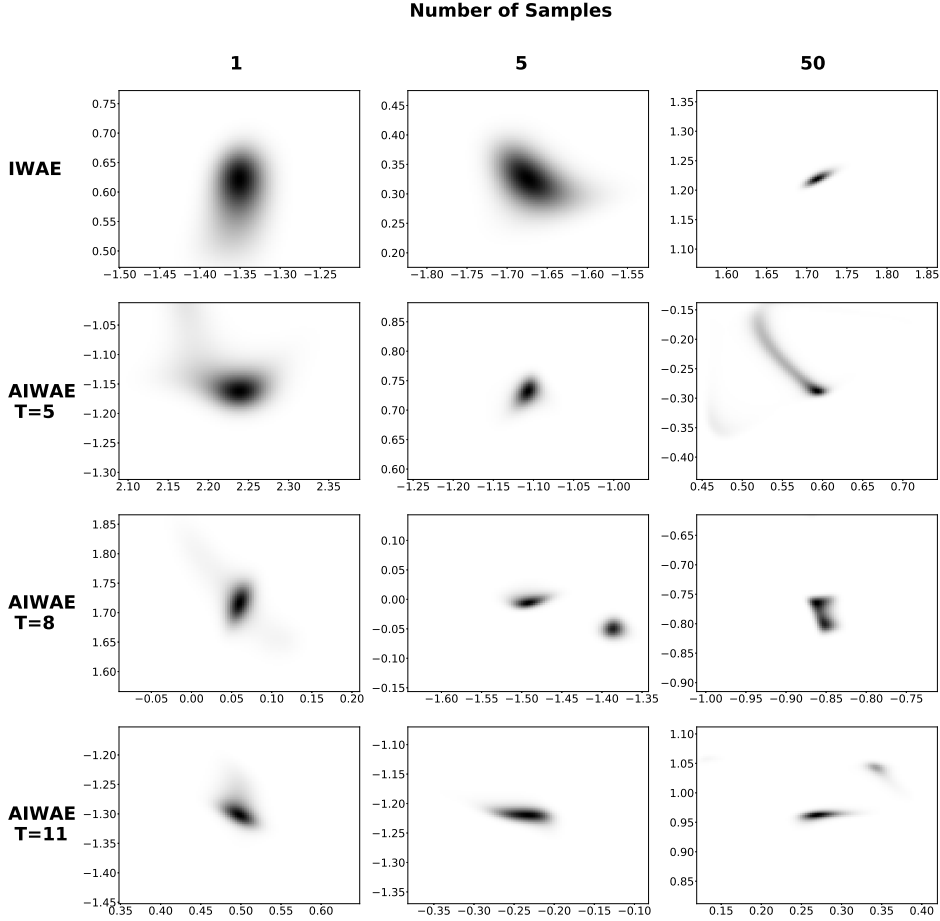


Figure S0: Posterior distribution $p_\theta(z|x)$ for a digit 0.

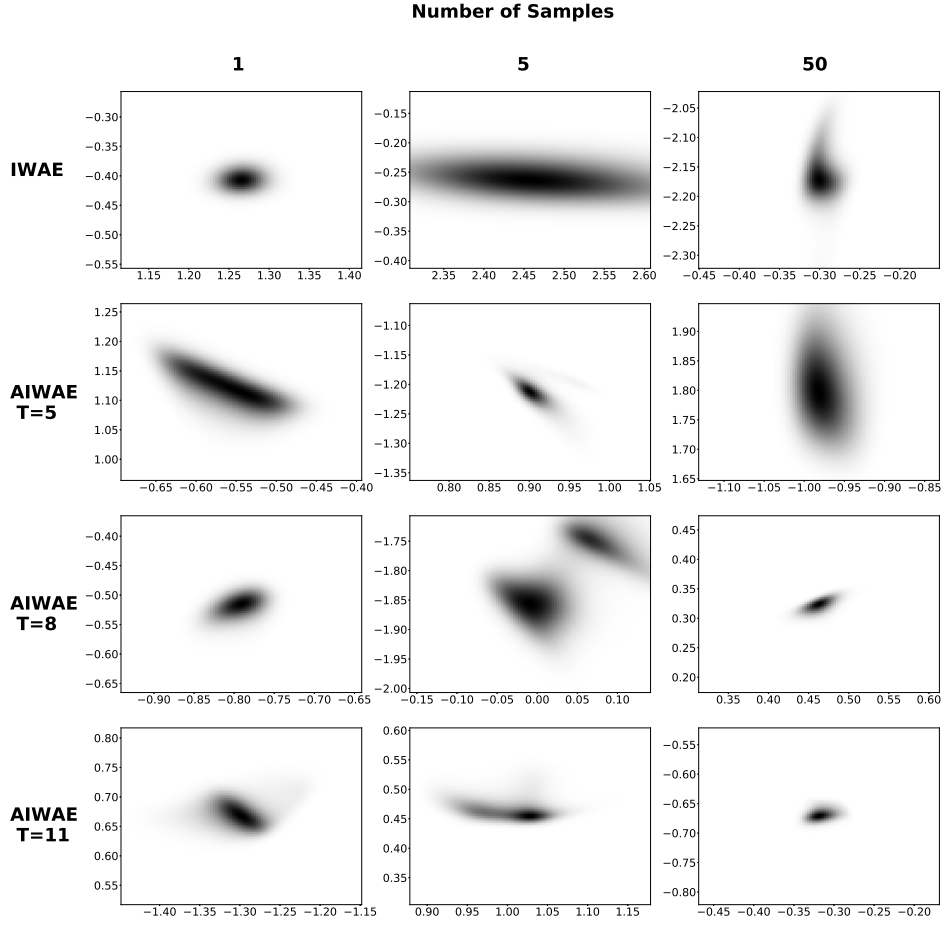


Figure S1: Posterior distribution $p_{\theta}(z|x)$ for a digit 1.

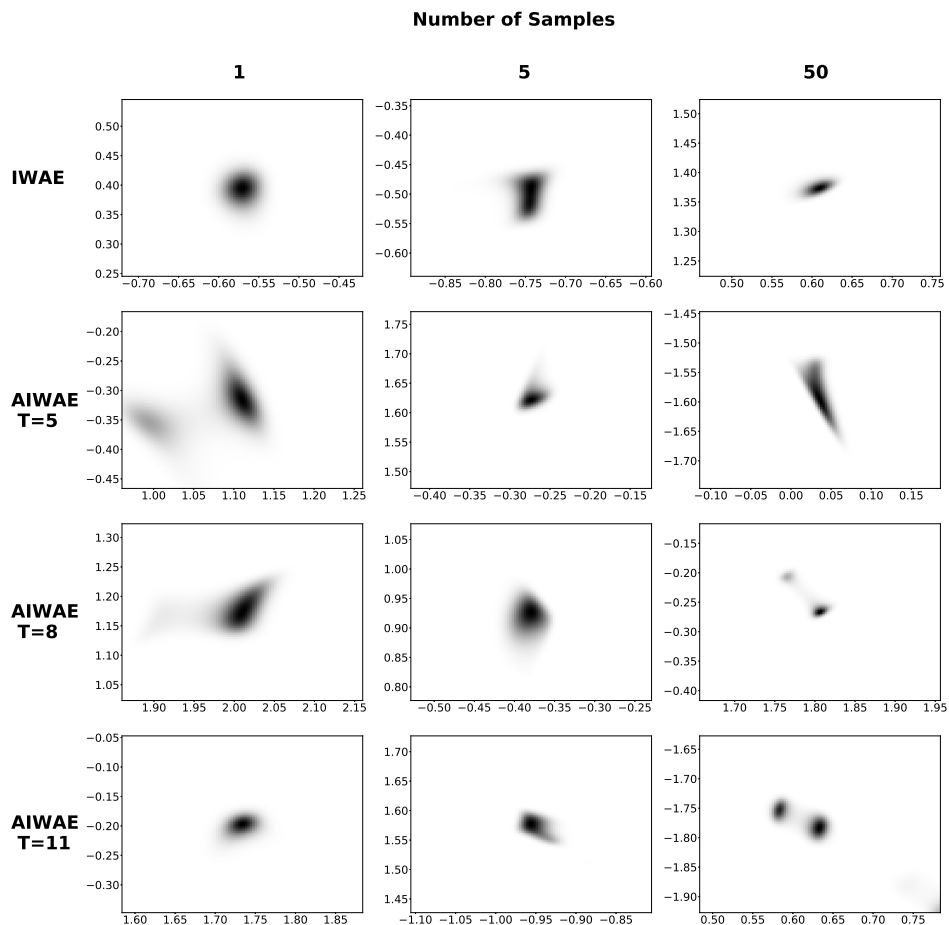


Figure S2: Posterior distribution $p_{\theta}(z|x)$ for a digit 2.

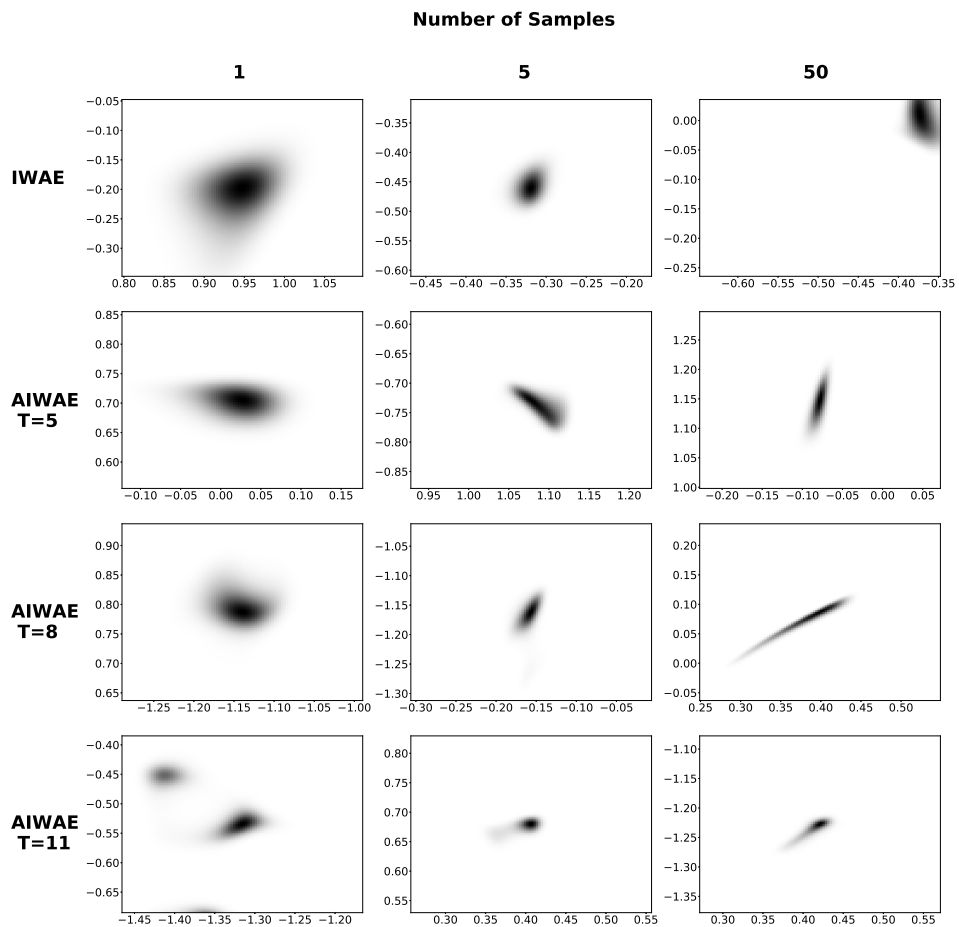


Figure S3: Posterior distribution $p_{\theta}(z|x)$ for a digit 3.

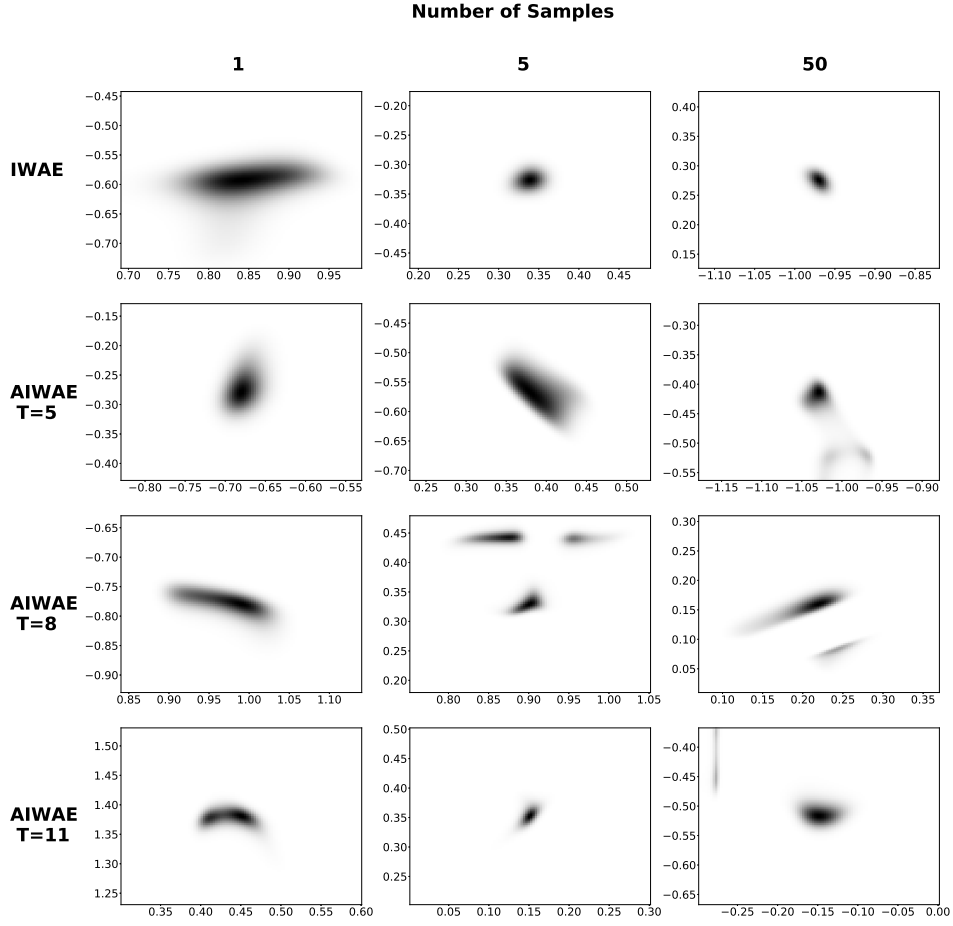


Figure S4: Posterior distribution $p_{\theta}(z|x)$ for a digit 4.

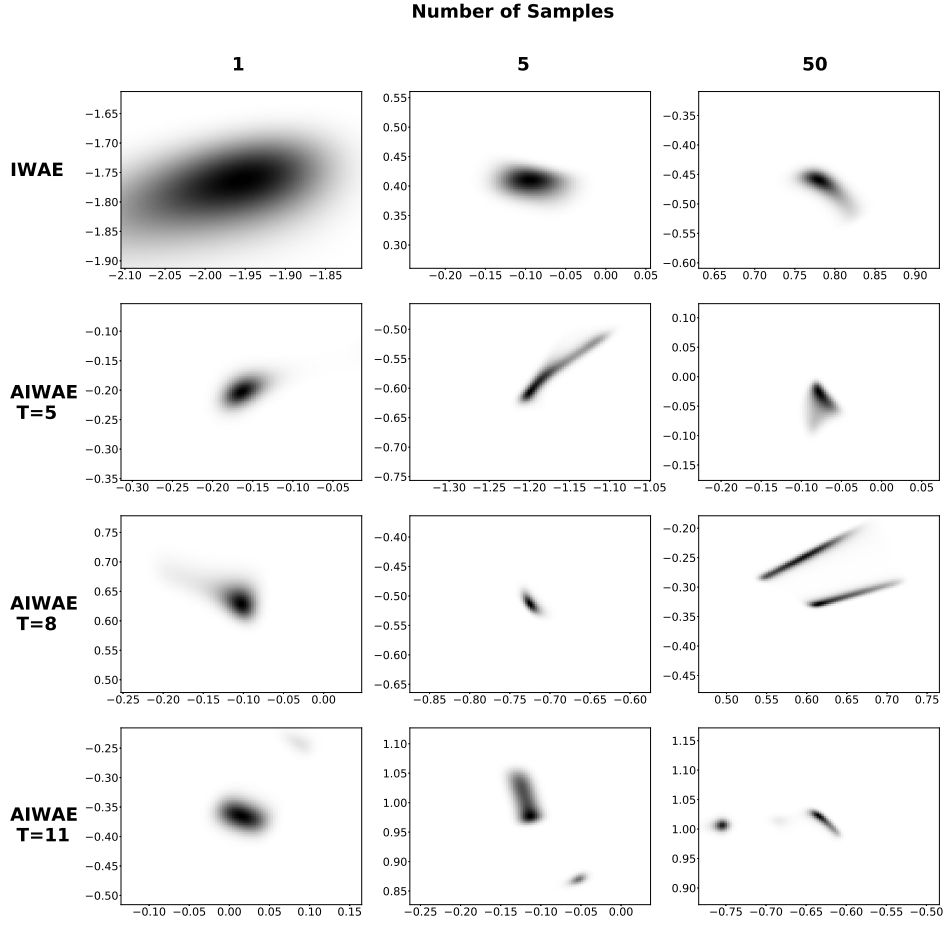


Figure S5: Posterior distribution $p_{\theta}(z|x)$ for a digit 5.

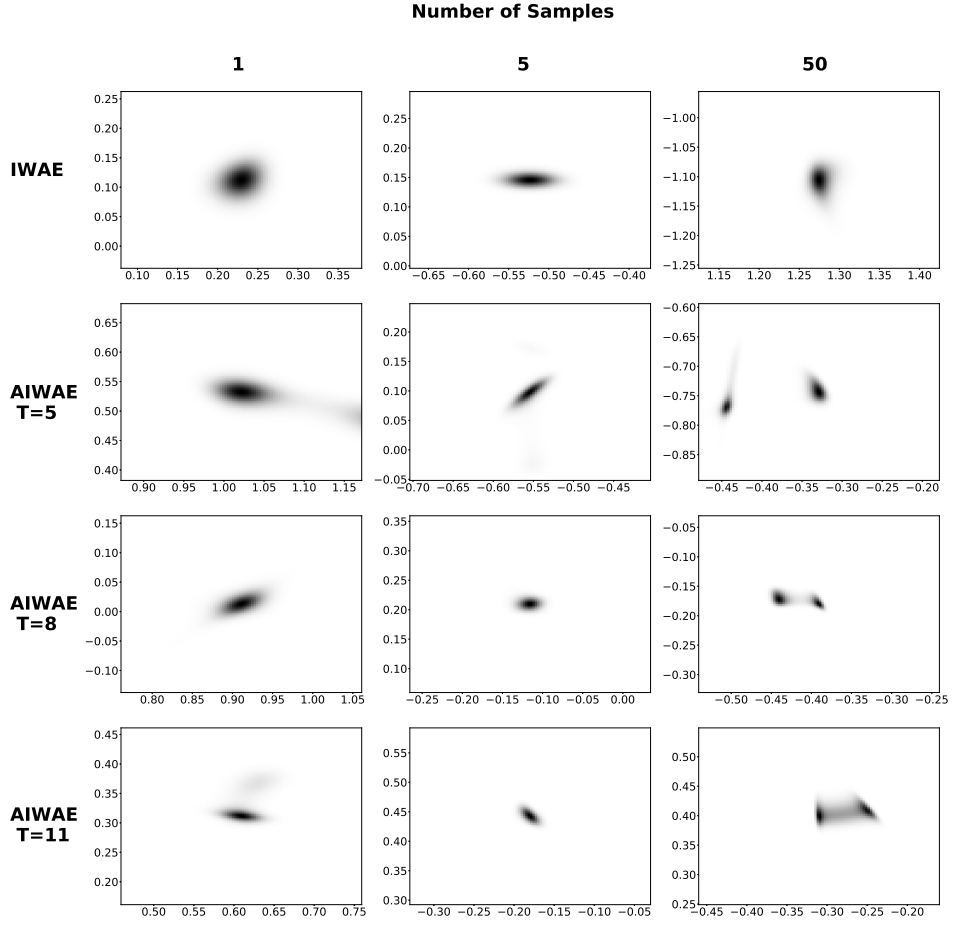


Figure S6: Posterior distribution $p_{\theta}(z|x)$ for a digit 6.

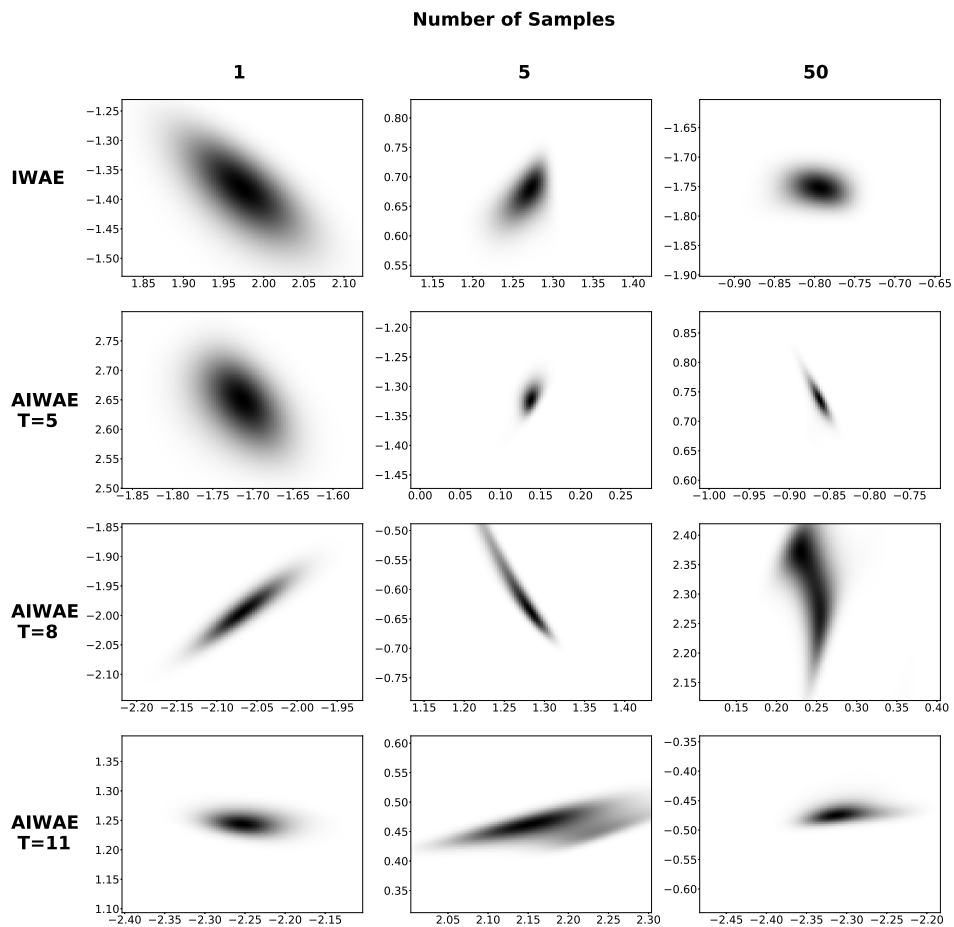


Figure S7: Posterior distribution $p_{\theta}(z|x)$ for a digit 7.

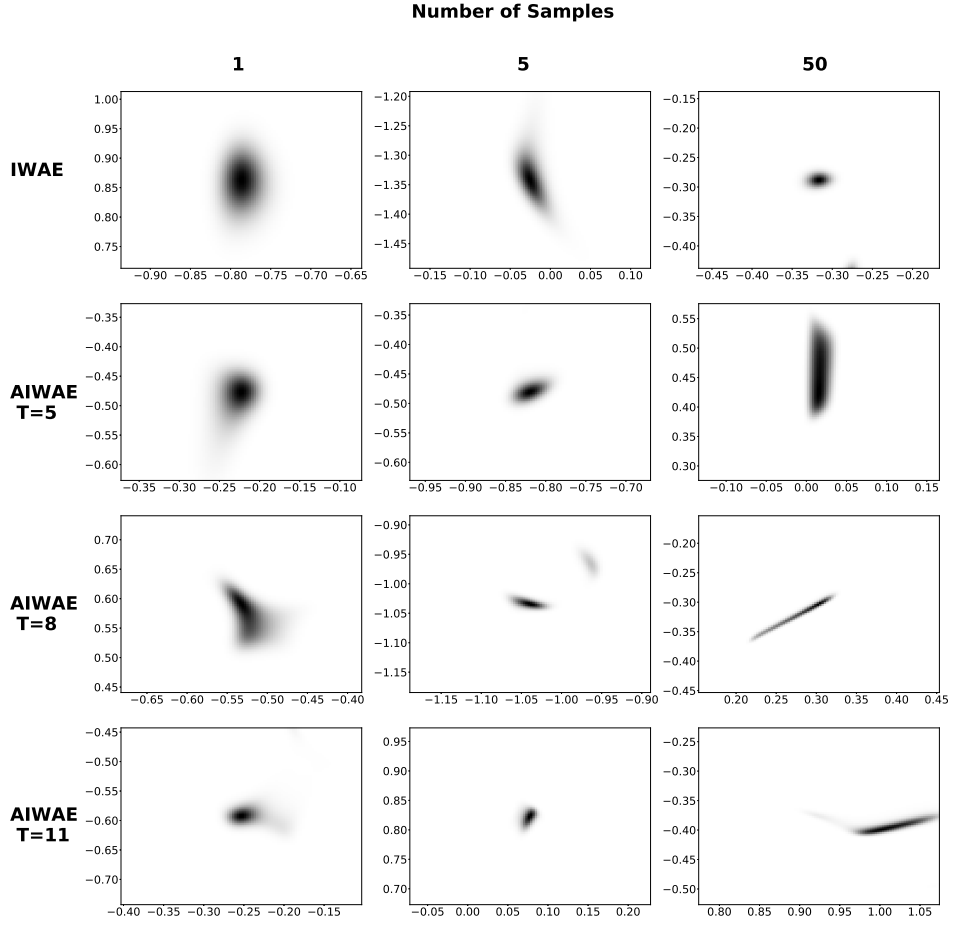


Figure S8: Posterior distribution $p_{\theta}(z|x)$ for a digit 8.

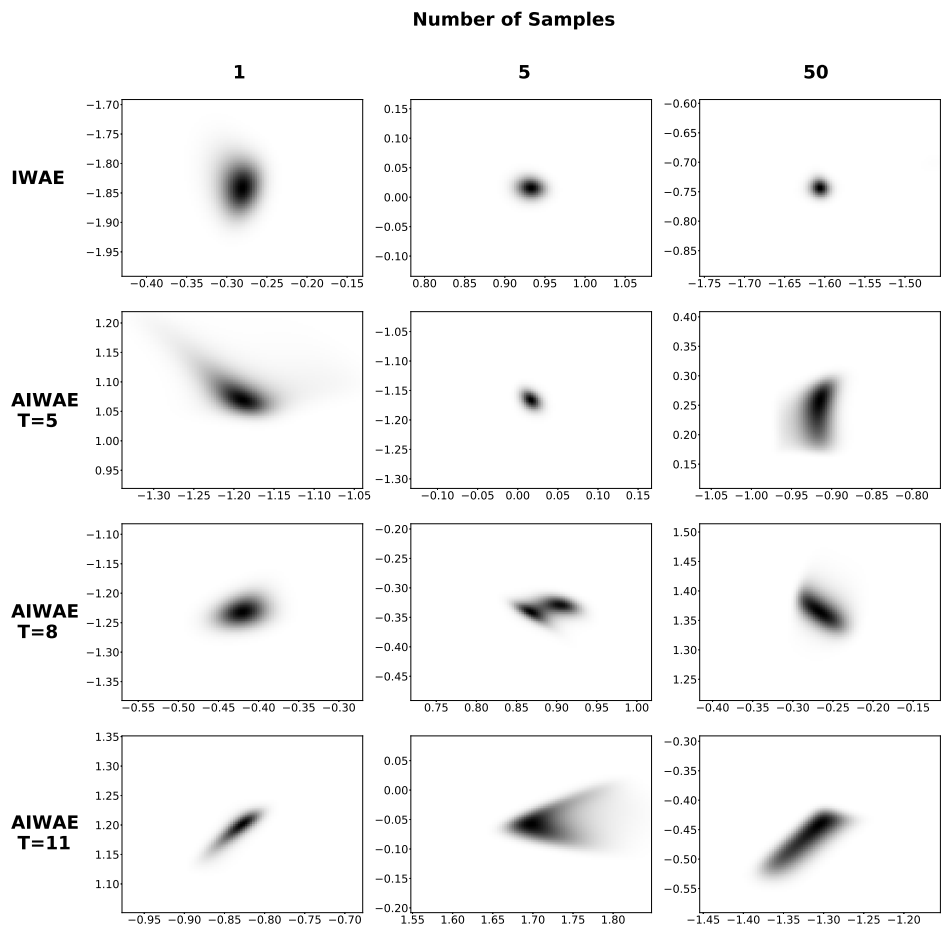


Figure S9: Posterior distribution $p_{\theta}(z|x)$ for a digit 9.

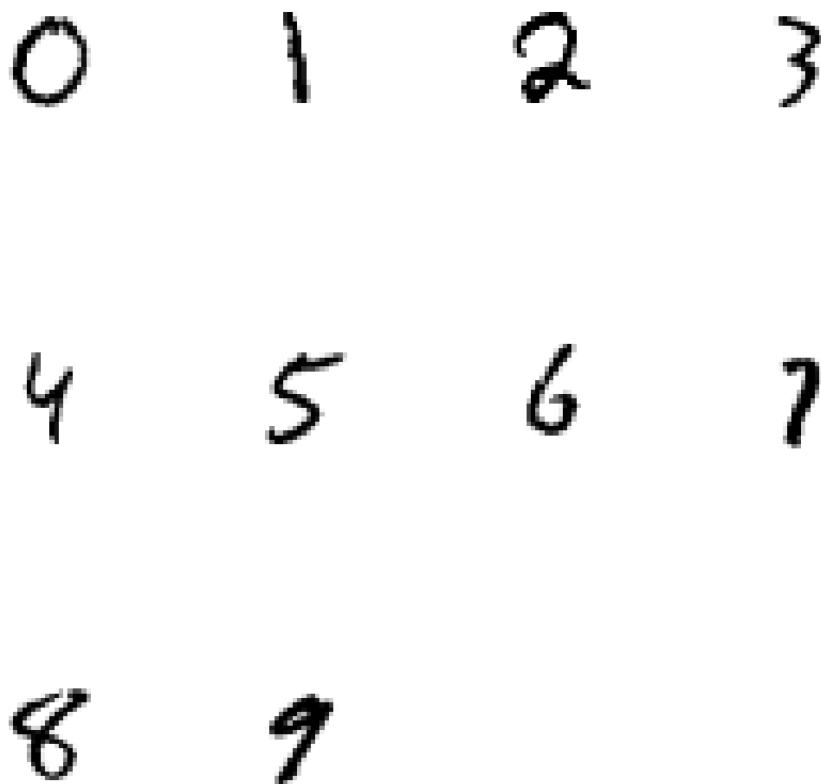


Figure S10: Digits used to calculate the posterior distributions $p_{\theta}(z|x)$ shown in Figures S0-S9.